



# Vibration spectroscopy of water on stepped gold surfaces

Harald Ibach \*

*Institute for Bio- und Nano-Systems (IBN3), Jülich Forschungszentrum, D 52425 Jülich, Germany*

## ARTICLE INFO

### Article history:

Received 27 August 2009

Accepted for publication 26 November 2009

Available online 29 November 2009

### Keywords:

Water

Ice

Stepped surfaces

Gold

Vibration spectroscopy

## ABSTRACT

The vibration spectrum of H<sub>2</sub>O (ice) adsorbed at low temperatures on Au(1 0 0), Au(1 1 1), and Au(1 1 5) is studied using electron energy loss spectroscopy. On the Au(1 0 0) surface, the spectra show the presence of the typical H-bonded network of water molecules for all coverages from the submonolayer into the multilayer range. The absence of a non-H-bonded OH-stretching mode is indicative for the “H-down bilayer”. On stepped surfaces, on the other hand, a considerable fraction of the H-atoms remains in the non-H-bonded state; surprisingly even in the multilayer range, and even after annealing. The fraction of non-H-bonded hydrogen atoms scales with the step density. Spectral features of water adsorbed at step-sites are isolated after annealing a surface exposed to small doses of H<sub>2</sub>O. The results are discussed in the context of recent theoretical studies as well as in conceivable relation to the experimentally found reduction of the Helmholtz-capacitance on stepped Au(1 1 *n*) electrodes.

© 2009 Elsevier B.V. All rights reserved.

## 1. Introduction

This work was motivated by recent surprising results on the capacitance of Au(1 1 *n*) electrodes in HClO<sub>4</sub>-electrolytes [1]. It was found that the concentration-independent part of the total capacitance, the so-called Helmholtz-capacitance or inner-layer capacitance is dramatically reduced on stepped surfaces. On the Au(1 1 5) surface e.g., the Helmholtz-capacitance amounts to only 54% of the Helmholtz-capacitance on Au(1 0 0). Essentially two effects contribute to the Helmholtz-capacitance: the electronic polarizability of the metal and the structure of water, in particular the stratification of liquid water, near a solid surface [2]. Since the electronic polarizability of metal surfaces tends to increase with the step density because of the higher flexibility of electrons at steps [3] the reduction of the Helmholtz-capacitance must be attributed to the structure of water and possibly to a reduced polarizability of water which may result from the structure of water adjacent to the surface.

The structure of liquid water, in particular the stratification of liquid water next to electrode surfaces has been studied in situ and under potential control using grazing incidence X-ray scattering. Unfortunately, only a few experiments are known. The experimental data of the first work of that kind had forced the authors to assume an unphysical high density of water molecules near the surface [4,5] which may have discouraged researchers from further endeavors until lately [6]. Stepped surfaces have not found attention in this regard. The same holds for theory. However, theory has recently advanced to a point where structural and elec-

tronic properties of water at the liquid–solid interface can be addressed without resorting to model potentials [7,8]. An extension to stepped surfaces is possible but has not yet been performed [9].

In the absence of theory and as experiments on the structure of liquid water at stepped surfaces may prove even more difficult than on flat surfaces, studies on the solid form of water (ice) at stepped surfaces may be useful as an intermediate step to elucidate the strange behavior of the Helmholtz-capacitance. The ice-like form of water is readily obtained in ultra-high vacuum by adsorbing water at low temperatures and has therefore been studied extensively in the past (for a review on the early work see [10]). Concerning the structure, it is universally agreed that water molecules, if adsorbed as molecules in the temperatures range of 80–150 K, aggregate to form hexagonal bilayers. In a single complete bilayer, 75% of the hydrogen atoms are engaged in hydrogen-bonds between the oxygen atoms. The remaining 25% may provide bonding to a second bilayer or, in case of a single bilayer, remain in a non-H-bonded (NHB) state. Variants of the original model for a single bilayer proposed in 1980 [11] differ in the placement of these NHB-hydrogen atoms. From the vibration spectra, Ibach and Lehwald concluded that on reconstructed Pt(1 0 0) surfaces the NHB-hydrogen atoms partly establish a hydrogen type bond to the metal surface [11] as was observed earlier for CH-species [12]; other NHB-hydrogen atoms stick out from the bilayer as dangling OH units. Bilayers with all three H-atoms of a ring that are not engaged in H-bonding pointing upwards and downwards from the outer three oxygen atoms are noted as “H-up” and “H-down” bilayers, respectively. Theoretical studies on Au(1 1 1), Ag(1 1 1), Pt(1 1 1) and Pd(1 1 1) find nearly equal binding energies for “H-up” and H-down bilayers with a slightly higher binding energy for the latter [8,13]. Partial dissociation such as to bond the surplus hydrogen

\* Tel.: +49 0241 527793; fax: +49 02461 613907.

E-mail address: [H.Ibach@fz-juelich.de](mailto:H.Ibach@fz-juelich.de)

atoms directly to the surface has been considered for Ru(0 0 0 1) surfaces [14,15].

The present work is a study of the vibration spectrum of water adsorbed at  $\sim 140$  K on Au(1 0 0), Au(1 1 1) and Au(1 1 5) surfaces using electron energy loss spectroscopy (EELS). For all three surfaces, the spectra display the well-known vibration signature of water bi- and multilayers, respectively. The sharp OH-stretching mode at around  $3700\text{ cm}^{-1}$ , which is characteristic for NHB-hydrogen, is completely absent for Au(1 0 0) at any coverage. It is, however, present on the stepped surfaces. The intensity of the NHB-mode scales with the step density. Most remarkably, roughly the same relative intensity of the NHB-mode is observed from a single bilayer up to ten bilayers. Furthermore, the NHB-mode survives prolonged annealing of the water layers up to the desorption temperature. This indicates that on stepped surfaces it is steric impossible to simultaneously establish bonds to the surface and engage all hydrogen atoms in H-bonds as on flat surfaces. This result may be relevant also for the metal/liquid–water interface. Spectral features of water bonded to step-sites were obtained after dosing the surface with small amounts of water, in particular after moderate annealing of the surface. The spectra are discussed in terms of models for the structure of water on flat and stepped surfaces.

## 2. Experimental

Experiments were performed in an ultra-high vacuum chamber equipped with a cylindrical mirror Auger-spectrometer, low energy electron diffraction (LEED) and an electron energy loss spectrometer (EELS) of the latest type [16,17]. The base pressure in the system was below  $1 \times 10^{-11}$  mbar, i.e. below the sensitivity limit of our ion gauge. Gold crystals were cut from a single crystal rod by spark erosion and polished to the desired orientation within  $0.1^\circ$ . The crystal disks were mounted on the cold stage of a liquid-nitrogen cooled manipulator by means of tantalum wire loop and three fixtures made from thin tantalum sheet metal. Temperature was controlled via a 0.1 mm diameter Ni–NiCr thermocouple squeezed between the gold sample and the fixtures. A wound tungsten wire at the back side of the crystal served to heat the sample, if so desired, while the sample was immersed into the EELS scattering chamber and while spectra were recorded (with some loss of intensity depending on the AC-heating current). Annealing within a temperature/time frame just below desorption was thereby achieved in a controlled manner. Cooling stage and crystal are electrically isolated from ground such as to permit the application of a tunable potential for the compensation of possible work function changes following exposure to water. In this way the electrode potentials of the EELS-spectrometer can be left as they were adjusted for optimum reflection from the clean surface. For the Au(1 0 0) surface, a shallow maximum in the intensity was typically obtained after raising the voltage on the sample by a few tenths of a volt, indicating a small increase in the work function of the sample upon adsorption of water.

The gold crystals were cleaned by sputtering with  $\sim 3\text{ }\mu\text{A cm}^{-2}$  of 1 keV argon ions. Initial sputtering time was 1 h to remove the layer that was damaged by the polishing procedure. For renewed cleaning of the surface after a day of experiments 15 min of sputtering sufficed. Sputtering was followed by a flash to 1100 K and 30 min annealing at temperatures gradually falling from 950 K to 800 K. After cooling to room temperature, the LEED pattern of Au(1 0 0) surface exhibited the characteristic spots of the reconstruction. On the reconstructed surface the topmost layer consists approximately of a hexagonal close packed layer with a higher atom density by about 25% which is incommensurate with the substrate because of a slight rotation by about  $0.81^\circ$  with respect to the [1 1 0]-direction [18]. In contrast, the Au(1 1 5) surface remains

unreconstructed [19] and displays the characteristic spot splitting of stepped surfaces. Steps on the Au(1 1 1) surface tend to aggregate in bunches of (1 1 5) to (1 1 7) orientation leaving larger reconstructed terraces between steps [20]. Scanning tunneling microscope (STM) images of the reconstruction-induced corrugation on these terraces show that the periodicity of the reconstruction is enlarged compared to the (1 0 0) surface and that the corrugation is oriented exactly along  $\langle 1\ 1\ 0 \rangle$  [20].

Exposure to water was performed with the sample placed near the water vapor inlet with the sample kept at  $\sim 140$  K. Water doses ranged from 0.08 to  $10 \times 10^{-6}$  mbars. As a matter of convenience we denote in the following  $1 \times 10^{-6}$  mbars as 1 L (1 L = 1 Langmuir, originally defined as  $1 \times 10^{-6}$  Torr). The ion gauge calibration factor of water is practically identical to that of air [21]. The dose of  $1 \times 10^{-6}$  mbars of water according to the ion gauge reading therefore corresponds to a surface exposure of  $3.5 \times 10^{14}$  water molecules per  $\text{cm}^2$ . The sticking coefficient of water at low temperatures is one at all coverages [10]. Since the density of water molecules in a bilayer is about  $5 \times 10^{14}\text{ cm}^{-2}$ , an exposure of 1.4 L yields a surface coverage equivalent to a single bilayer. Exposures of the sample were performed with a fixed time of 100 s (time interval between opening and closing the valve) while the pressure was varied to obtain the required doses. After closing the leak valve the water pressure fell off exponentially with a time constant of 30 s. The actual water exposures are therefore larger than the nominal exposures by 30%. Hence, 1 L nominal exposure corresponds approximately to one complete bilayer. Nominal exposures are quoted in the following. Test experiments with doses produced with exposure times extended by a factor of five and pressures reduced accordingly by a factor of 5 yielded indistinguishable spectra.

Energy loss spectra were mostly taken with impact energies of 7 eV. The energy was chosen for maximum reflectivity on the stepped surfaces for which the elastic beam is rather broadly distributed. The nominal resolution in direct beam without the additional broadening due to the angular spread of the electrons after reflection from the surface was  $60\text{ cm}^{-1}$  ( $\sim 7.5\text{ meV}$ ). Exposures below 1 L were also studied using 4 eV impact energy and a nominal resolution of  $30\text{ cm}^{-1}$  ( $\sim 4.5\text{ meV}$ ). All spectra are recorded in the direction of elastic reflection. The angles of incidence measured from the normal were about  $66^\circ$ ,  $80^\circ$  and  $60^\circ$  for the Au(1 0 0), the Au(1 1 1) and the Au(1 1 5) crystals, respectively. Partly because of the different scattering angles, yet primarily because of the large differences in the angular distribution of the elastic beam, the intensities of the vibrational losses obtained for the three surfaces cannot be compared on a quantitative level. Electron multiplier pulses were sampled in energy intervals of  $5\text{ cm}^{-1}$  and with gate time of 1–5 s.

## 3. Results

The key results of this study are shown in Figs. 1–3 with the spectra of Au(1 0 0), Au(1 1 1) and Au(1 1 5) obtained after 1 L, 3 L, and 10 L exposure to water vapor. The 1 L spectrum of Au(1 0 0) (Fig. 1) displays the classic four spectral features of a well-ordered bilayer: the OH-stretching mode of hydrogen engaged in H-bonding at  $3390\text{ cm}^{-1}$ , a weak hydrogen scissor mode at  $1630\text{ cm}^{-1}$ , the hydrogen bending mode at  $730\text{ cm}^{-1}$  (frustrated rotation around an axis perpendicular to the  $C_2$ -axis of the  $\text{H}_2\text{O}$  molecule, frequently denoted as libration mode), and an oxygen mode at  $240\text{ cm}^{-1}$ . Annealing of the crystal up to 160 K further increased the order of the water layer as evidenced by the elastic intensity which increased by a factor of two. The spectrum as such is not affected however. The two humps at  $1460\text{ cm}^{-1}$  and  $4100\text{ cm}^{-1}$  are double losses of the  $730\text{ cm}^{-1}$  and a combination

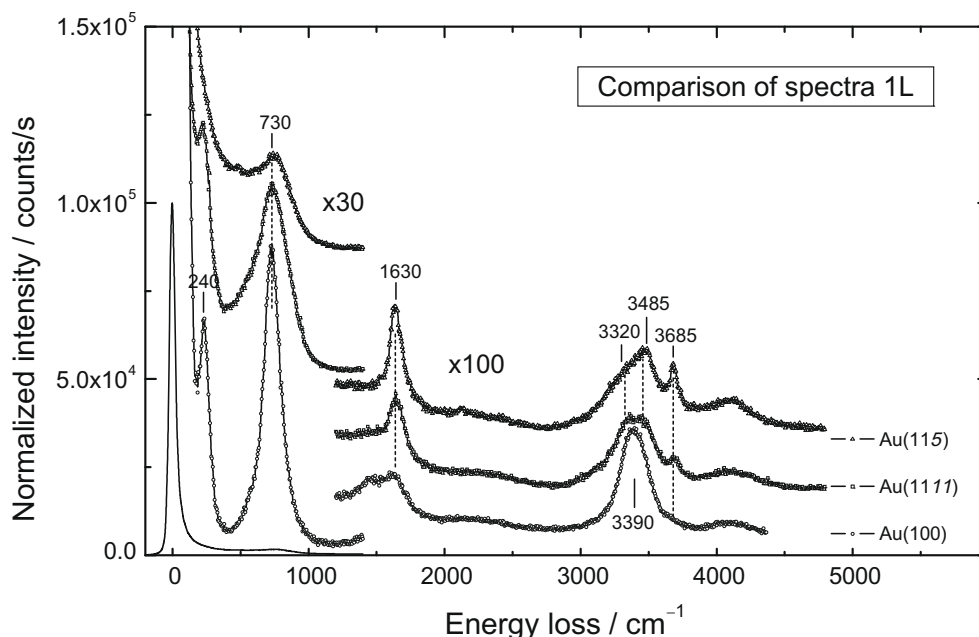


**Fig. 1.** Energy loss spectra of Au(1 0 0), Au(1 1 1) and Au(1 1 5) surfaces after dosing with 1 L of water at 140 K. The elastic peak is that of the Au(1 1 5) surface, normalized in intensity to  $1 \times 10^5$  counts/s. The magnifications 30 $\times$  and 100 $\times$  refer to the elastic line of that surface. The wave numbers indicated in the stretching regime were obtained by fitting to a set of Lorentzians.

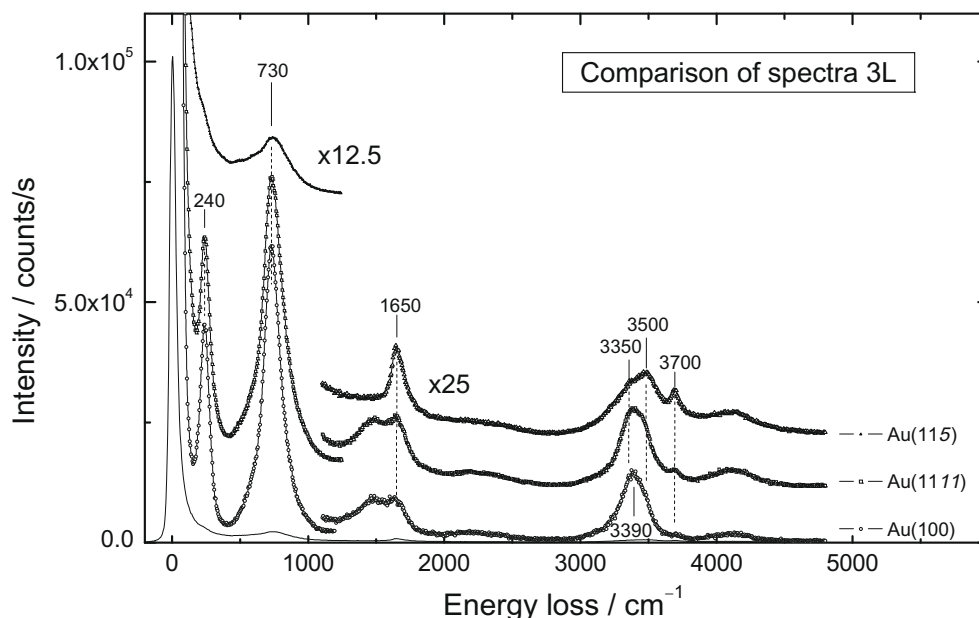


**Fig. 2.** Energy loss spectra of Au(1 0 0), Au(1 1 1) and Au(1 1 5) surfaces after dosing with 3 L of water at 140 K. The elastic peak is that of the Au(1 1 5) surface, normalized in intensity to  $1 \times 10^5$  counts/s. The magnifications 12.5 $\times$  and 25 $\times$  refer to the elastic line of that surface. The wave numbers indicated in the OH-stretching regime were obtained by fitting to Lorentzians.

loss of the  $3390\text{ cm}^{-1}$  and  $730\text{ cm}^{-1}$  bands, respectively. Such multiple losses are typical for intense dipole scattering features [22] and need no further consideration in the context of this paper.

With increasing step density the spectrum changes in a characteristic way. Most notably is the appearance of the sharp stretching mode of non-H-bonded (NHB) hydrogen at  $3685\text{ cm}^{-1}$ . Concomitant with the appearance of the NHB-mode is the higher intensity and the sharpening of the scissor mode at  $1630\text{ cm}^{-1}$ . The libration mode at  $730\text{ cm}^{-1}$  broadens and the OH-stretching regime of H-bonded hydrogen (HB-hydrogen) develops some structure. The structure may be decomposed by fitting four Lorentzians of vari-

able width (one for the multiple loss around  $4100\text{ cm}^{-1}$  that is of no concern otherwise). The fitting procedure yields a broad loss (FWHM:  $170\text{ cm}^{-1}$ ) at  $3320\text{ cm}^{-1}$ , another broad loss (FWHM:  $95\text{ cm}^{-1}$ ) at  $3485\text{ cm}^{-1}$ , and a sharp loss at  $3685\text{ cm}^{-1}$  (Fig. 1).

The spectra for higher coverages change very little save for an increase in the intensities with respect to the elastic beam (Figs. 2 and 3). Most remarkably, the relative intensity of the NHB-mode to the HB-modes in the OH-stretching regime is practically independent of coverage. This means that the fraction of broken H-bonds in thicker layers (equivalent to 3 and 10 bilayers) remains roughly the same as in a single bilayer. The high intensity of the

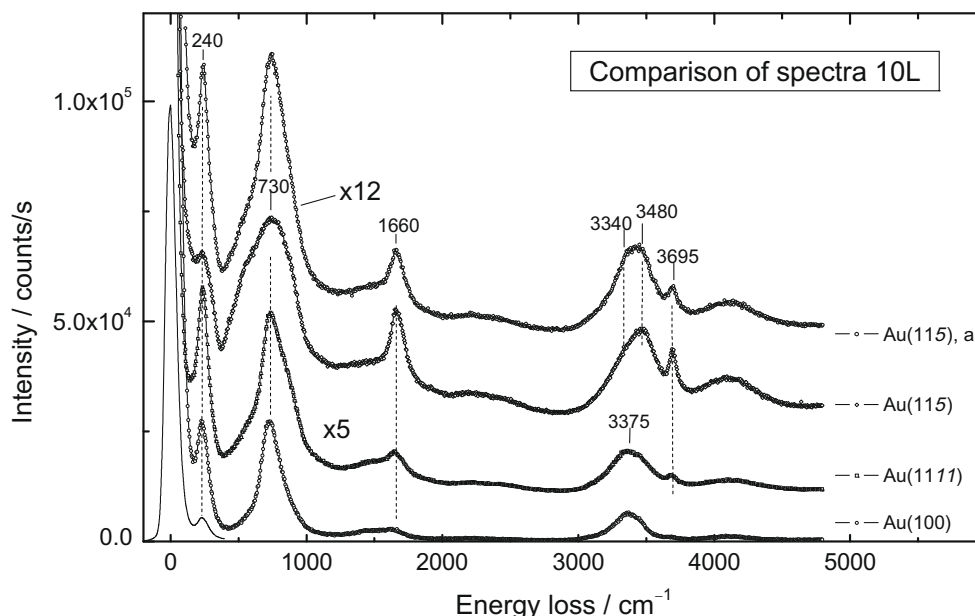


**Fig. 3.** Energy loss spectra of Au(1 0 0), Au(1 1 1) and Au(1 1 5) surfaces after dosing with 10 L of water at 140 K. The wave numbers indicated in the OH-stretching regime were obtained by fitting to Lorentzians. The elastic peak is that of the Au(1 1 5) surface, normalized in intensity to  $1 \times 10^5$  counts/s. Also shown is a spectrum (denoted by “a”) of the Au(1 1 5) surface after annealing to 165 K for 20 min. The higher magnification factor for the latter case (12 $\times$ ) is because the ordering caused by annealing raises the intensity of the elastic peak that falls into the small angular aperture of the spectrometer. The inelastic intensity is less affected since the angular distribution of energy losses is intrinsically broader.

NHB-stretching mode cannot be removed by annealing. As an example out of numerous attempts with different annealing temperatures Fig. 3 shows the effect of 20 min annealing to 165 K which is just below the desorption temperature. The intensity of the NHB-hydrogen mode relative to the HB-mode reduces only slightly. Simultaneously, the libration mode sharpens and increases in intensity. The annealing process also increases the elastic intensity that falls into the angular aperture of the spectrometer which shows an improved ordering of the water layer. The inelastic intensity is less affected since the angular distribution of energy losses is intrinsically broader. The intensity of inelastic peaks relative to the elastic peak therefore reduces upon ordering. A higher magnification factor of 12.5 is therefore employed in the presentation of the spectrum obtained after annealing.

Fig. 4 shows the spectra in the coverage range below one bilayer. The spectral features differ from the bilayer case in two ways. The spectrum develops distinct structures in the low frequency range and the relative intensity of the NHB-stretching mode is even larger. In order to make that statement quantitative the OH-stretching regime was fitted with four Lorentzians (one for the multiple loss around  $4100 \text{ cm}^{-1}$ ). The procedure yields the resonance frequencies, the amplitudes and the widths for each peak. The ratio of the integrated intensity of the NHB-hydrogen band (amplitude  $\times$  width) divided by the integrated intensity of the band due to HB-hydrogen vs. exposure is shown in Fig. 5a. The ratio starts from about 0.23 at the lowest coverage to level off at about 0.1 in the monolayer and multilayer range. A small further reduction to 0.08 is obtained by prolonged annealing at 165 K (see Fig. 3). Fig. 5a furthermore shows the intensity ratio on Au(1 1 1) and Au(1 1 5) surfaces for 1 L exposure. Within the error margin the ratio scales with the step density. The NHB-hydrogen is therefore attributed to water at steps. Fig. 5b shows the intensity of HB- and NHB-stretching bands on Au(1 1 5) referenced to the elastic peak as function of the dose (squares and circles, respectively).

The dashed line represents the slope of 1 in the log–log plot. The relative intensity of the HB-band increases proportional to the

dose, regardless of the coverage. This is consistent with a sticking coefficient of one even in the multilayer range. The same has been observed for most other water adsorption systems [10]. The smaller slope of the NHB-peak is due to the smaller fraction of NHB-hydrogen at higher coverages. The additional spectral features in the low frequency regime are presumably to be attributed to a form of water that is specific to steps. Previous STM studies of water on Pt(1 1 1) and Au(1 1 1) have shown that water at steps binds more tightly to the surface, hence desorbs at higher temperatures than water on terraces [23,24]. We have therefore attempted to isolate the step specific form of water by annealing. A selection of the results of several efforts is shown in Fig. 6. In these experiments the resolution was set to  $3.75 \text{ meV}$  in direct beam. The resolution degrades to  $4.4 \text{ meV}$  in the elastic reflected beam because of the larger angular divergence of the beam entering the analyzer. Although the elastic reflected beam was still at an intensity level of  $2 \times 10^5$  counts/s, the inelastic intensity is significantly reduced because of the broadness of the spectral features and because of the smaller angular aperture angle that comes with the lower pass energies in the energy dispersive deflectors. To compensate partly for the lower count rates in the inelastic channels the spectra in Fig. 6 were recorded with a time span of 5 s per  $5 \text{ cm}^{-1}$  channel. In order to be able to identify possible spectral features in the tail of the elastic peak, the decay of the elastic peak of the clean surface was fitted to a double-exponential which was then subtracted from the spectra of surfaces covered with water. The upper spectrum in Fig. 6 was obtained after deposition of 0.1 L water at 139 K. The resulting spectrum is similar to the spectrum shown in Fig. 4 for 0.15 L. A peak at about  $640 \text{ cm}^{-1}$  appears in addition to the libration mode of bilayer water at  $730 \text{ cm}^{-1}$ . Upon annealing to 160 K and 165 K for 5 min the intensity at  $730 \text{ cm}^{-1}$  decreases while the intensity of the loss at  $640 \text{ cm}^{-1}$  remains largely unaffected. The frequency of that mode shifts down to about  $610 \text{ cm}^{-1}$  upon annealing. The surface was then dosed again with 0.15 L water and annealed to 170 K for 5 min. The  $610 \text{ cm}^{-1}$  loss is now the dominant feature in the spectrum. Its intensity is also reduced compared to the spectra above. Roughly

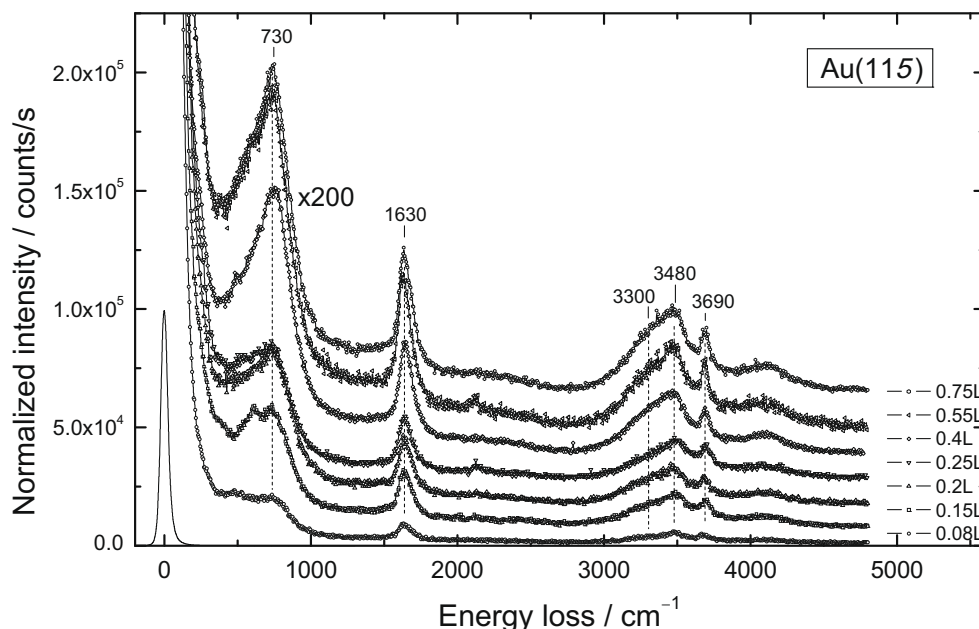


**Fig. 4.** Energy loss spectra of Au(115) in the low coverage regime after exposure at 140 K. Spectra are sampled with 5 s per channel. All spectra have the same magnification with respect to the elastic peak which is normalized to  $1 \times 10^5$  counts/s. Doses are listed at the end of each spectrum. The wave numbers indicated in the stretching regime were obtained by fitting to four Lorentzians (one for the double loss).

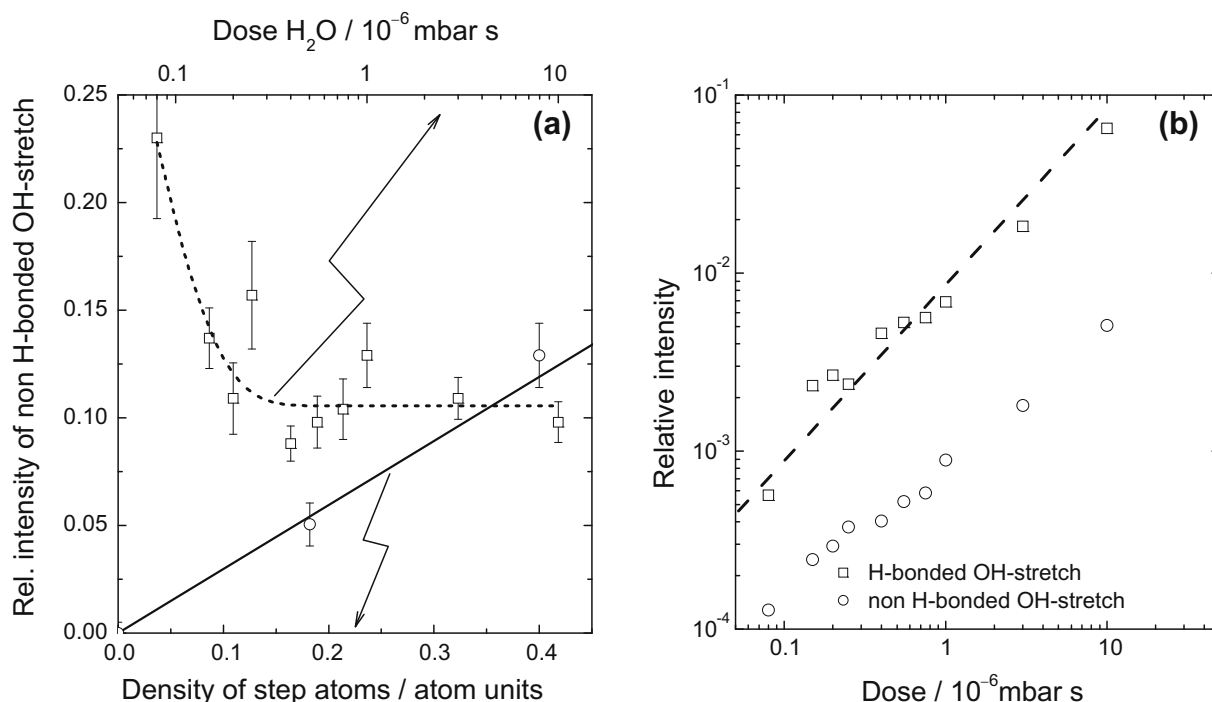


**Fig. 5.** (a) Intensity of the NHB-band divided by the intensity of the HB-band as function of the dose on Au(115) and as function of step density for 1 L exposure (upper and lower scale, respectively). (b) Intensity of HB- and NHB-stretching bands on Au(115) referenced to the elastic peak as function of the dose (squares and circles, respectively). The dashed line represents the slope of 1 in the log-log plot. The intensity of the HB-band therefore rises linearly with the dose in agreement with a sticking coefficient of one at all coverages. The smaller slope of the NHB-band indicates a smaller fraction of NHB-hydrogen at higher coverages.

the same spectrum albeit at again a lower intensity level is obtained after dosing a clean surface with 0.15 L of water followed by an annealing to 175 K for 2 min. Longer heating at the same temperature leads to complete desorption. The presence of the H<sub>2</sub>O scissor mode ( $1630 \text{ cm}^{-1}$ ) and of HB and NHB-modes in the OH-stretching regime (Fig. 6) proves that the  $610 \text{ cm}^{-1}$  mode is to be attributed to

water. Fitting of the OH-stretching regime with two Lorentzians (dashed lines in Fig. 6) yields peak positions of  $3510 \pm 5 \text{ cm}^{-1}$  (HB-mode) and  $3695 \pm 5 \text{ cm}^{-1}$  (NHB-mode). The NHB-mode has the same frequency as for the unannealed surfaces (Fig. 4) while the HB-mode appears at a higher frequency. The broad band at  $3300 \text{ cm}^{-1}$  (Fig. 4) is missing completely. The intensity ratio of



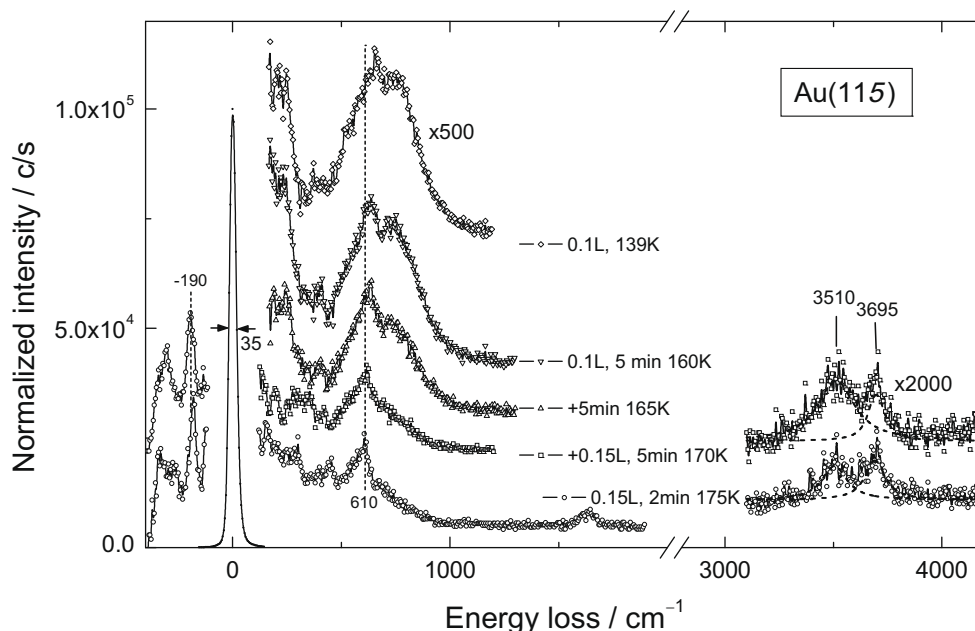


**Fig. 6.** Energy loss spectra of the Au(115) surface in the low coverage regime after subtraction of a double exponential tail simulating the spectrum of a clean (115) surface. From top to bottom: Spectrum after dosing with 0.1 L at 139 K (diamonds), the same after annealing to 160 K for 5 min (triangles top up), additional exposure to 0.15 L at 140 K with subsequent annealing to 170 K for 5 min (squares), spectrum after dosing with 0.15 L at 140 K after annealing to 170 K for 2 min (circles). Also shown are the OH-stretching bands with the signatures of HB- and NHB-features for the last two spectra.

the NHB-mode and the HB-band is much higher than for the unannealed surface ( $0.33 \pm 0.04$  and  $0.95 \pm 0.15$  for the second lowest and the lowest spectrum in Fig. 6, respectively).

The results prove the existence of a step specific form of water characterized by modes at  $610 \text{ cm}^{-1}$ ,  $1630 \text{ cm}^{-1}$ ,  $3510 \text{ cm}^{-1}$  and  $3690 \text{ cm}^{-1}$ . Furthermore, a low frequency mode at about  $190 \text{ cm}^{-1}$  can be discerned as an energy gain on the left hand side of the elastic peak. The mode cannot be observed as an energy loss because the more intense tailing of the elastic peak on the energy loss side which results from electrons that are scattered from the sample at larger angles, in particular due to the steps and the elastic diffuse scattering from adsorbed water.

## 4. Discussion

### 4.1. Water on Au(100)

We first consider the spectrum obtained for a nominal 1 L exposure which according to our calibration should correspond approximately to a water coverage that is equivalent to one complete bilayer. The 1 L spectrum of Au(100) (Fig. 1) indeed shows the four spectral features of a well-ordered bilayer: the OH-stretching mode of hydrogen engaged in H-bonding at  $3390 \text{ cm}^{-1}$ , a weak hydrogen scissor mode at  $1630 \text{ cm}^{-1}$ , the hydrogen libration mode at  $730 \text{ cm}^{-1}$ , and an oxygen mode at  $240 \text{ cm}^{-1}$ . There is no indication of a NHB-stretching mode. The observed high intensity of the specular reflected beam as well as the further increase of that intensity after annealing the surface to 160 K calls for a well ordered structure of the water layer.

In a perfectly ordered single bilayer of water 1/2 hydrogen atom per oxygen molecule cannot engage in H-bonding. These H-atoms either point inwards from the outer oxygen atoms towards the Au-surface to realize the so-called H-down configuration (Fig. 7a) or point outwards (H-up configuration, Fig. 7b). Since the NHB-hydrogen atoms in the H-up configuration would give rise to a large dynamic dipole moment of the NHB-stretching mode one can exclude the H-up configuration from the absence of a spectral feature

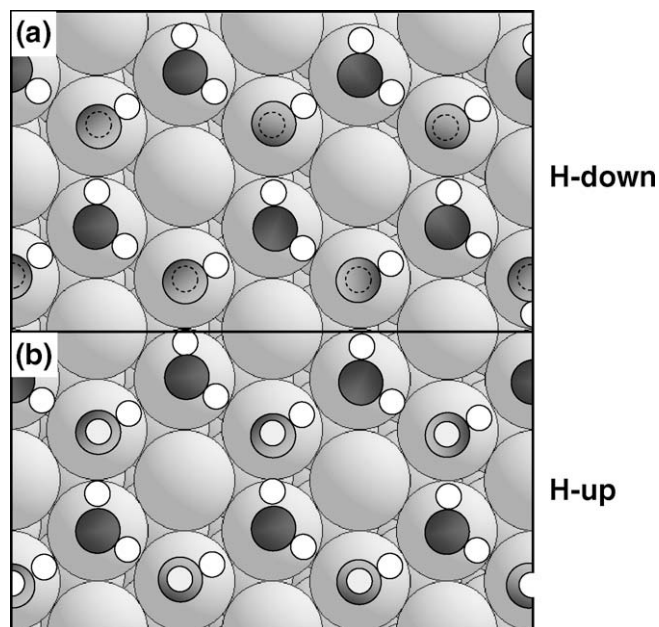


**Fig. 7.** Top view on an idealized (111) surface (large grey shaded balls) covered with an ideally ordered bilayer of water. Oxygen atoms are shown as medium sized balls in dark grey and light grey for the lower and upper oxygen atoms in the bilayer, respectively. Three quarters of the hydrogen atoms are engaged in H-bonding. The remaining H-atoms are bonded to the upper oxygen atoms. They point downwards to the surface and upwards to realize the H-down and H-up configuration, respectively (dashed circles and small light grey balls in Fig. 7a and b, respectively).

around  $3700 \text{ cm}^{-1}$ . This conclusion is in agreement with recent theoretical studies of Schnur and Groß [8] and Meng et al. [13]. Both authors find for Au(111) a  $\sim 4\%$  higher binding energy for water in the H-down configuration. For the H-down configuration, the NHB-mode is invisible because the dipole moment of the mode

is screened and/or because the frequency is red-shifted and broadened as for a genuine H-bonding between oxygen atoms. Theoretical studies of Meng et al. suggest the frequency of H-down hydrogen to be strongly red-shifted on Pt(1 1 1), Pd(1 1 1), and Rh(1 1 1), although not on Au(1 1 1) [13,25]. For Au(1 0 0), the NHB-mode remains absent even for ten bilayers (Figs. 2 and 3). This shows that the water multilayers entertain a (nearly) perfect network of hydrogen-bonds as in ice crystals.

A remarkable feature of the spectrum of a single bilayer on Au(1 0 0) is the low number of dipole active modes. Only two dipole active hydrogen bending modes are discernable, the libration mode at  $730\text{ cm}^{-1}$  and the scissor mode at  $1630\text{ cm}^{-1}$ . This is in stark contrast to water on Pt(1 1 1) [26]. There are two possible explanations. One is that the effective symmetry of the bilayer is  $C_{6v}$  rather than  $C_{3v}$  [27]. In other words, the structurally different two water molecules in the rings have the (nearly) same spectrum of bending modes. The other possibility is that only the bending modes of one type of water molecules, e.g., of the lower one, are associated with a considerable dynamic dipole moment. In any case, the high intensity of the bending mode at  $730\text{ cm}^{-1}$  compared to the scissor mode at  $1630\text{ cm}^{-1}$  indicates a rather flat orientation of the water molecules consistent with the bilayer model.

Au(1 0 0) surfaces prepared in ultra-high vacuum are always reconstructed. The reconstruction is not lifted by water adsorption. The high effective symmetry of the water layer, be it  $C_{6v}$  or  $C_{3v}$ , therefore calls for a small substrate–water interaction. This is likewise consistent with theory. Meng et al. calculate the bond energy of water monomers to Au(1 1 1) to 105 meV per molecule, as opposed to 291 meV on Pt(1 1 1). The binding energy per water molecule in the bilayer structure differs much less (454 meV on Au(1 1 1) vs. 534 meV on Pt(1 1 1)). Considering that each water molecule in the bilayer structure is bonded by 1/2 Au–O bond this means that on gold surfaces the Au–O bond contributes 12% to the total binding energy per molecule whereas it is 27% on platinum. There are indications that the mismatch between the structure of the reconstructed Au(1 0 0) surface and the bilayer reduces the substrate–water interaction even further. On Au(1 1 1), theory and experiment place the libration mode at  $845\text{ cm}^{-1}$  and  $835\text{ cm}^{-1}$ , respectively, i.e. much higher than the  $730\text{ cm}^{-1}$  found here [13,28]. A frequency of  $730\text{ cm}^{-1}$  is characteristic for ice multilayers on Au(1 1 1) and elsewhere [10,28]. The characteristic change in the frequency as one moves from a single bilayer to multilayers that is observed on Au(1 1 1) is absent for Au(1 0 0) (Figs. 1–3). Hence the first bilayer is hardly affected by the presence of gold.

As remarked earlier, a slight increase in the work function upon adsorption of water is indicated by the magnitude and sign of the bias on the sample required for optimum signal recovery after adsorption of water. A small increase in the work function is also consistent with the H-down configuration since Schnur and Groß calculate the work function change due to water on Au(1 1 1) to +0.5 eV and −1.5 eV for H-down and H-up bilayer, respectively.

In summary, the analysis of the experimental spectra and comparison to theory provides evidence for a well-ordered bilayer structure in the H-down configuration on Au(1 0 0). The buckling and the atom density of the reconstructed Au(1 0 0) surface appears to have little effect on the structure and properties of the bilayer.

#### 4.2. Water on stepped surfaces

Water spectra of the stepped surfaces differ in several aspects from Au(1 0 0). The  $730\text{ cm}^{-1}$  libration mode is broader, the scissor mode at  $1630\text{ cm}^{-1}$  more intense, the OH-stretching regime appears to consist of several discernable modes, and most strikingly the spectra display a sharp OH-stretching mode of NHB-hydrogen.

The intensity of the latter scales with the step density (Fig. 5a), and so does the intensity of the scissor mode. Spectra of Au(1 1 5) at low exposures (Fig. 4) reveal a distinctly separate H-bending mode below  $730\text{ cm}^{-1}$ . Mild annealing of the surface causes the  $730\text{ cm}^{-1}$ -mode to nearly disappear and to single out the lower H-bending mode at  $610\text{ cm}^{-1}$ . The broad structure in the OH-stretching regime around  $3300\text{ cm}^{-1}$  likewise disappears to leave a comparatively narrow OH-stretching band of HB-hydrogen at  $3510\text{ cm}^{-1}$  which is more than  $100\text{ cm}^{-1}$  higher than the HB-modes on the Au(1 0 0) surface. The two bands at  $610\text{ cm}^{-1}$  and  $3510\text{ cm}^{-1}$  together with the scissor mode at  $1630\text{ cm}^{-1}$  and the NHB-stretching mode at  $3695\text{ cm}^{-1}$  are therefore to be attributed to a water species that exists only on stepped surfaces. This form of water presumably possesses only a single type of hydrogen-bonds (because of the narrowness of the band) and a type of hydrogen-bond that is distinct from the hydrogen-bonds in the bilayer rings (because of the higher frequency). Furthermore the ratio of NHB-hydrogen to HB-hydrogen should be larger than for a complete bilayer (1 L exposure).

A special form of water at steps on Pt(1 1 1) surfaces has been found experimentally by Morgenstern et al. [23]. Morgenstern et al. showed that water is more strongly bound at steps compared to water at terraces. A decoration of steps at low doses of water was also observed by Morgenstern [24]. Meng et al. studied theoretically the adsorption of water at (1 1 0)(1 0 0)-steps (“A-steps”) on Pt(1 1 1) [13]. They found that water monomers have a much higher binding energy at the top of step atoms compared to terrace atoms (449 meV vs. 291 meV). The preferred structure of water at steps on Pt(1 1 1) is a H-bonded zigzag chain with every Pt-step atom covered by one water molecule. The H-atoms not engaged in H-bonding point alternatively outwards and inwards with respect to the step edge. According to Meng et al. the binding energy per water molecule in that configuration (480 meV) is almost as high as the binding energy in a complete bilayer network (534 meV). The high binding energy of water at step atoms is consistent with the qualitative picture of the bonding of water via the doubly occupied oxygen  $p_z$  orbital (lone-pair orbital). The dative bond of oxygen requires the presence of empty states near the Fermi-level in the substrate. The position on the top of a step atom is a site of high binding energy as it is most depleted of electrons compared to other sites (which may be considered as a type of Smoluchowski-effect [29]). For the same reason water binds preferentially with the oxygen on top of a substrate atom and the HOH-plane is nearly parallel to the surface [30,31].

#### 4.3. Structure models

In the following, the observed spectral features of water on stepped surfaces are discussed in terms of models for the structure. Since there appears to be no principle difference in the spectra of Au(1 1 1) and Au(1 1 5) other than the intensities of features that are characteristic for stepped surfaces we focus the discussion on the Au(1 1 5) surface which is neither faceted nor reconstructed [19] and consists of a sequence of steps and terraces, each 2.5 atoms wide, on the average. Fig. 8 shows a top view of the ideal (1 1 5) surface together with three propositions for the structure of water which take the general understanding of water bonding as well as the observed spectral features into account. Large grey balls represent gold atoms, the small balls oxygen atoms. Hydrogen atoms are not shown. Unlike the Au(1 0 0) surface, the Au(1 1 5) surface is not reconstructed [32]. A perfect match of the water bilayer structure to the surface structure can therefore not be achieved, even in the absence of steps. One might consider the possibility that NHB-hydrogen might become visible in the spectrum just because of the change in the structure of the gold terraces. However, there are three arguments against that proposition. One is the approximate

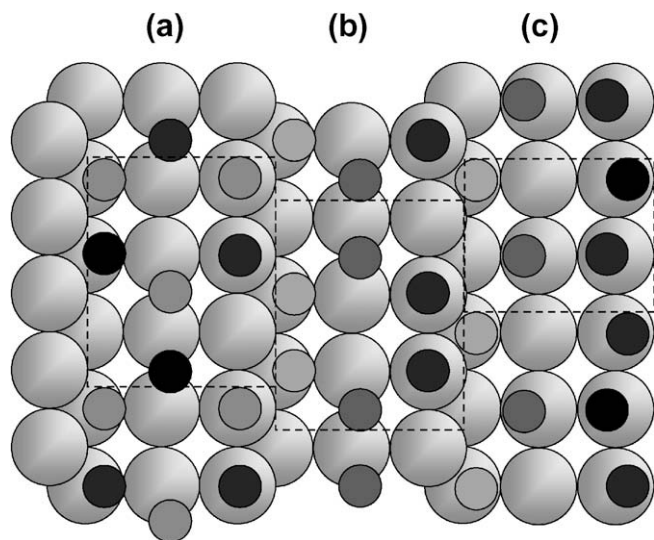


**Fig. 8.** Three models for water on Au(1 1 5). Large grey balls represent gold surface atoms, the small balls oxygen molecules. Hydrogen atoms are not shown. Dashed lines are the unit cells. All models place a large fraction of the oxygen atoms on the step atoms as these are sites of highest binding energy. Model (a) retains the buckling of the bilayer as on flat surfaces. Model (b) introduces a buckling that reflects the position with respect to the substrate atoms. Model (c) is based on the zigzag chain structure of water at steps proposed for platinum [13].

linear relation between the intensity of the NHB-stretching mode and the step density (Fig. 4a). The continuing increase in the intensity of the NHB-stretching mode in the multilayer range is a second one. Both experimental results point towards the step-sites as the (main) source of NHB-hydrogen. Finally, the bonding of the water bilayer to the gold substrate is much weaker than the bonds between the water molecules (see Section 4 above). A mismatch between the gold structure and the bilayer structure can therefore not lead to a breaking of H-bonds between water molecules. One can however not exclude the possibility that some of the H-atoms not engaged in H-bonding point upwards on stepped surfaces rather than downwards as on the reconstructed Au(1 0 0) surface. This is why hydrogen atoms are not shown in Fig. 8. Model (a) retains the bilayer structure with high and low lying oxygen atoms. The size of the ring is as in Fig. 7 where it is matching the ideal Au(1 1 1) surface. The hexagonal rings are rotated to fit to the size of the terraces as well as to bring as many oxygen atoms into the favored position on top of step atoms. In Fig. 8b oxygen atoms in equivalent positions have the same shade to indicate that their height above the surface may reflect the type of surface site. In Fig. 8c the step atoms are decorated with the water zigzag chain as proposed for steps on Pt(1 1 1). The structure is continued onto the terraces as a distorted hexagonal network of oxygen atoms.

In all three models the bilayer rings are distorted and involve water molecules that are bonded to the surface with different strength. Hence the models are consistent with the broader appearance of the spectral feature as described above. For all three models, the distance between oxygen atoms residing on two adjacent terraces is too large to allow hydrogen-bonding across the steps. Thus all models necessarily produce NHB-hydrogen. Assuming that the hexagonal rings still adsorb in the H-down configuration, two hydrogen atoms per ring, thus two per three step atoms, would be non hydrogen-bonded in case of models 8a and 8b. In case of 8c it would be one NHB-hydrogen every second step atom. It should be noted that more NHB-hydrogen atoms may result from a possible flip from the H-down into the H-up configuration, which is cannot be excluded in view of the small energy difference on flat surfaces.

Experimentally, the intensity of the NHB-stretching mode is correlated with the intensity of the scissor mode. This suggests that the observed scissor mode on stepped surfaces has to be attributed to NHB-hydrogen and that the scissor mode which involves a NHB-hydrogen atom carries a higher dipole moment than the scissor mode of HB-hydrogen. Whether or not the models can account for the higher dipole moment is not known at present.

The conversion of the low coverage experimental spectra upon annealing is most easily explained with model 8c. The specific spectral features described above would then be attributed to the zigzag chains of water. Only one particular type of hydrogen-bonding exists in this structure consistent with the narrowness of the OH-stretching band and the higher frequency. The model is presumably also consistent with the intensity ratio of NHB-modes to the HB-modes which is of the order of 1 for step water and 0.1 for the bilayer. The ratio of the number of NHB-atoms to HB-atom in the chain model is 1. Making the reasonable assumption that one hydrogen atom per unit cell (note the smaller unit cell of model 8c) is in the H-down position the corresponding ratio is 2:5, i.e. smaller than for the chain.

Model 8c, or variants of it, is most attractive as it combines the possibility for a consistent qualitative interpretation of all experimental result with past experience of theoretical studies on platinum surfaces. In view of the much lower binding energy between oxygen and gold an alternative class of models should also be considered in which AuO-bonds are traded-in for hydrogen-bonds. The model would involve a complete lateral network of H-bonds as on flat surfaces. To make that possible, some of the oxygen atoms, presumably those at the lower edge of the steps, have to give up their AuO-bonds by raising their height enough to be able to establish a H-bond with the oxygen atoms residing on top of step atoms. A model of that type which uses the structure units of Fig. 8b is illustrated in Fig. 9. Alternatively, one might base a 2D H-bonding network on the structural elements of Fig. 8c. However, the resulting gross deviations of the HOH bond angles make such a structure less likely. In order to make the model as shown in Fig. 9 compatible with experiment one would have to assume (i) that the bilayer realizes the H-up configuration (to account for the observed NHB-stretching mode) and (ii) that annealing at low coverage restructures the water layer significantly such as to reveal the observed spectral features of that state.

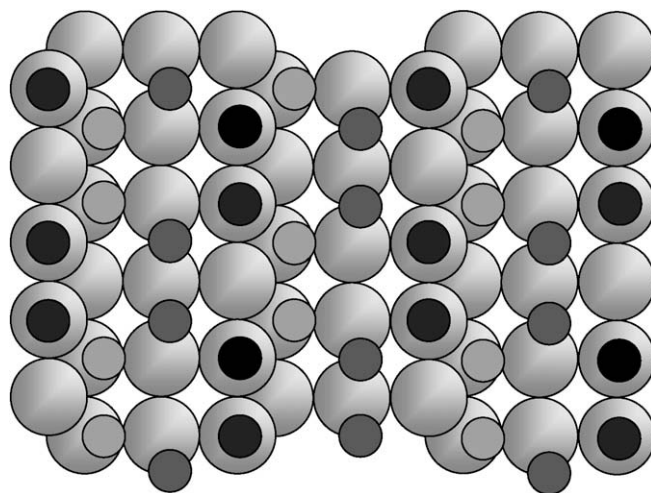


**Fig. 9.** Model for water on Au(1 1 5) surfaces featuring a complete network of lateral hydrogen-bonding. In order to achieve that, the oxygen atoms at the bottom of the steps (depicted in light grey) need be moved upwards to bring them into a H-bonding distance to the oxygen atoms on top of the step atoms (depicted in black). The distance of the light grey atoms to the surface is then too large for an oxygen lone-pair bonding to the substrate.



#### 4.4. Multilayers of water on stepped surfaces

The proposed models are now discussed in view of the development of the spectra for multilayer exposures (Figs. 2 and 3). We consider models as depicted in Fig. 8 first. For all the three cases a–c the pseudo-hexagonal rings on each terrace can serve as a template for the growth of multilayers of a wurtzite ice structure. The vertical displacement of the terraces, however, would introduce corresponding vertical displacements of the lattices grown on each terrace. The impossibility to interconnect the lattices by H-bonds would persist for thicker layers. This is consistent with a striking feature of the experiment namely that the 1 L spectrum of Au(1 1 5) and the unannealed 10 L spectrum of Au(1 1 5) are nearly identical except for the low frequency region. The partial disappearance of NHB-hydrogen upon annealing can be explained as structural rearrangements that allow for the establishment of more H-bonds at the interface between the crystals grown on different terraces.

Models based upon a more or less perfect first bilayer (Fig. 9) are less compatible with the development of spectra at higher coverage: In these models, the NHB-hydrogen stretching mode has to be attributed to hydrogen in the H-up position as shown in Fig. 7b. Concomitant with the growth of further layers the surface density of those hydrogen atoms would stay constant, while the surface density of HB-hydrogen would increase with coverage. This is at variance with Fig. 5b which shows that both, the relative intensity of HB-hydrogen and of NHB-hydrogen increases with coverage, the first one linearly, the latter one a little slower. The development of spectra at multilayer coverage therefore supports models of the type depicted in Fig. 8.

#### 5. Conclusions

Vibration spectra of water on Au(1 0 0) are consistent with the H-down bilayer model which is in agreement with theory. Striking differences in the spectra of water on stepped gold surfaces show that the bonding of solid water on stepped surfaces differs from Au(1 0 0) and other flat surfaces. A considerable fraction of hydrogen atoms cannot engage in H-bonding, neither in the first layer nor in the following layers. The spectra require further the existence of a special structure of water at steps. The large ratio of the intensities of the NHB- to the HB-stretching modes as well as the relatively high frequency of the HB-stretching mode are consistent with the zigzag chain model proposed for steps on Pt(1 1 1). Most likely candidates for models in the monolayer regime and above are those that combine elements of the chain model at steps with the bilayer structure as established for flat surfaces (Fig. 8c).

The striking differences in the spectra between stepped and flat surfaces at coverage beyond one bilayer are attributed to the impossibility to saturate simultaneously H-bonds and oxygen-surface bonds. As this impossibility is a consequence of the geometry of the surface, one might assume this fact to be relevant also for gold in contact with liquid water and thereby establish a possible

connection to the Helmholtz capacitance. On the other hand, Schnur and Groß have shown very recently that on Au(1 1 1) and Ag(1 1 1) the surface-oxygen distance distribution function of liquid water shows no indication at all for an oxygen-surface bond while such bonds do exist for platinum, palladium and rhodium [8]. The structure of the bilayer is likewise not preserved in liquid water in contact with gold. It therefore remains open whether or not the results presented in this paper may eventually contribute to the understanding of the interface between stepped surfaces and liquid water.

#### Acknowledgements

Inspiring discussion with Guillermo Beltramo on the metal/electrolyte interface and his critical reading of the manuscript are gratefully acknowledged. The author is indebted to Udo Linke for the skillful preparation of the crystals as well as for his many useful advices. Partial support by the Fond der Chemischen Industrie is also acknowledged.

#### References

- [1] G. Beltramo, M. Giesen, H. Ibach, *Electrochim. Acta* 54 (2009) 4305.
- [2] W. Schmickler, D. Henderson, *Progr. Surf. Sci.* 22 (1986) 323.
- [3] H. Ibach, W. Schmickler, *Phys. Rev. Lett.* 91 (2003) 016106.
- [4] M.F. Toney, J.N. Howard, J. Richer, G.L. Borges, J.G. Gordon, O.R. Melroy, D.G. Wiesler, D. Yee, L.B. Sorensen, *Nature* 368 (1994) 444.
- [5] M.F. Toney, J.N. Howard, J. Richer, G.L. Borges, J.G. Gordon, O.R. Melroy, D.G. Wiesler, D. Yee, L.B. Sorensen, *Surf. Sci.* 335 (1995) 326.
- [6] M. Ito, M. Yamazaki, *Phys. Chem. Chem. Phys.* 8 (2006) 3623.
- [7] S. Izvekov, G.A. Voth, *J. Chem. Phys.* 115 (2001) 7196.
- [8] S. Schnur, A. Groß, *New J. Phys.* 11 (2009) 125003.
- [9] A. Groß, Private Communication.
- [10] P.A. Thiel, T.E. Madey, *Surf. Sci. Rep.* 7 (1987) 211.
- [11] H. Ibach, S. Lehwald, *Surf. Sci.* 91 (1980) 187.
- [12] J.E. Demuth, H. Ibach, S. Lehwald, *Phys. Rev. Lett.* 40 (1978) 1044.
- [13] S. Meng, E.G. Wang, S. Gao, *Phys. Rev. B* 69 (2004) 195404.
- [14] P. Feibelman, *Science* 295 (2002) 99.
- [15] J. Weissenrieder, A. Mikkelsen, J.N. Andersen, P.J. Feibelman, G. Held, *Phys. Rev. Lett.* 93 (2004) 196102.
- [16] H. Ibach, *J. Electr. Spectr. Related Phenom.* 64/65 (1993) 819.
- [17] H. Ibach, M. Balden, S. Lehwald, *J. Chem. Soc., Faraday Trans.* 92 (1996) 4771.
- [18] B.M. Ocko, D. Gibbs, K.G. Huang, D.M. Zehner, S.G.J. Mochrie, *Phys. Rev. B* 44 (1991) 6429.
- [19] M. Sotto, J.C. Boulliard, *Surf. Sci.* 214 (1989) 97.
- [20] M. Moiseeva, E. Pichardo-Pedrero, G. Beltramo, H. Ibach, M. Giesen, *Surf. Sci.* 603 (2009) 670.
- [21] S. Wagener, C.B. Johnson, *J. Sci. Instrum.* 28 (1952) 278.
- [22] H. Ibach, D.L. Mills, *Electron Energy Loss Spectroscopy and Surface Vibrations*, Academic Press, New York, 1982.
- [23] M. Morgenstern, T. Michely, G. Comsa, *Phys. Rev. Lett.* 77 (1996) 703.
- [24] K. Morgenstern, Private Communication.
- [25] S. Meng, L.F. Xu, E.G. Wang, S. Gao, *Phys. Rev. Lett.* 89 (2002) 176104.
- [26] K. Jacobi, K. Bedürftig, Y. Wang, G. Ertl, *Surf. Sci.* 472 (2001) 9.
- [27] H. Ibach, *Physics of Surfaces and Interfaces*, Springer, Berlin, Heidelberg, New York, 2006.
- [28] G. Pirug, H.P. Bonzel, *Surf. Sci.* 405 (1998) 87.
- [29] R. Smoluchowski, *Phys. Rev.* 60 (1941) 661.
- [30] J.E. Müller, J. Harris, *Phys. Rev. Lett.* 53 (1984) 2493.
- [31] J.E. Müller, in: H.P. Bonzel, A.M. Bradshaw, G. Ertl (Eds.), *Physics and Chemistry of Alkali Metal Adsorption*, vol. 57, Elsevier, Amsterdam, 1989.
- [32] M. Alshakran et al., Private Communication.